Mapana Journal of Sciences
2022, Vol. 21, No. 2, 37-58
ISSN 0975-3303|https://doi.org/10.12723/mjs.61.4

Development of Silane Functionalized ZnO Nanoparticles for Enhancing Anticorrosion Application

Geetha Mable Pinto* & Apoorva Devadiga†

Abstract

The effect of zinc oxide nanoparticles surface modified with N-[3-(Trimethoxysilyl)propyl]ethylenediamine (15.5 nm) on mild steel in 0.5M HCl at five different concentrations and temperatures has been studied using Electrochemical Impedance Spectroscopy (EIS) and Tafel polarization curves. Results show that the inhibition efficiency of synthesized mixed type of inhibitor increases up to 40˚C and then decreases because of both physical and chemical adsorption. The activation parameters calculated using Arrhenius plot confirmed chemical adsorption process. Adsorption process follows Langmuir adsorption isotherm and free energy of adsorption values proved the spontaneous adsorption of inhibitor on mild steel sample. Scanning electron microscopy (SEM) analysis also showed that the synthesized nanoparticle is efficient as corrosion inhibitor. Green synthetic method was adopted in synthesis of inhibitor by using Phyllanthus Emblica (Gooseberry) extract. The inhibitor was characterized by Fourier Transform Infra-red Spectroscopy (FT-IR) and X-Ray Diffraction techniques.

Keywords: ZnO-Silane, green synthesis, functionalization, corrosion, adsorption

*Department of Chemistry, St Agnes Centre for Postgraduate Studies and Research, Mangaluru, India; geetha@stagnescollege.edu.in
†Department of Chemistry, St Agnes Centre for Postgraduate Studies and Research, Mangaluru, India; apoorvasappu13@gmail.com

1. Introduction

The term Nano is derived from the Greek word "Nano's" which means smaller in size or dwarf. Nanoparticles are those solid materials or particulate dispersions with the size varying from 1nm to 100nm. The surrounding interfacial layer of nanomaterials is an integral part constituting ions, inorganic and organic molecules. Thus, nanoscience deals with the study, synthesis, characterization and applications of particles of size about 1-100nm. There are two modes of manufacturing of nanomaterials. They are bottom–up approach and top–down approach. The bottom–up approach uses the processes such as self-assembly, chemical synthesis, molecular beam epitaxy, nanoimprint lithography, roll-to-roll processing, and dip penlithography. The top–down approach, which is commonly adopted, utilizes lithographic and nonlithographic fabrication technologies [1, 2]. Nanotechnology plays a vital role in developing world and deals with the processes pertinent to physics, chemistry and biology with diverse applications such as fabric compounds, food processing, agriculture and also in medical field. The properties of nanoparticles (1-100nm) largely vary from other macro particles due to their larger surface area. The modification in structural, chemical, optical, electrical, mechanical and morphological properties of materials can be achieved by decreasing the particle size to nano scale. Thus nano-size shows larger applications in various fields in contrast to bulk materials [3]. The agglomeration is the major drawback of nanosize and large surface area and needs to be controlled. Now a days, nanotechnology is the growing field because of its simplicity in development of well-advanced products with improved latest characteristics and functions which are having vast advantages in most of the fields. Along with several industrial applications, nanoscience is having vital use in medicinal field, biotechnology and communication field, etc. Some other applications include chemical engineering, optics, cosmetics, generation of energy, high performance materials, pharmaceutics, astronomy, computing and electronic applications and even as military applications. Nano chemistry has a major advantage in diagnostic and treatment of brain tumour, Alzheimer's and plague in arteries [4]. Nanomaterials are surface functionalized so that they are

connected to organic matrix and thus to increase the stability. There are two different ways to achieve surface functionalization i.e, in situ functionalization and ex situ functionalization. In in situ method, functionalization is achieved during the synthesis of nanoparticles. In ex situ functionalization, nanoparticles are synthesized in the beginning after which functionalization is carried out. Functionalization can be achieved using the ligands like small molecules, surfactants, dendrimers, polymers, and biomolecules [5].

The advantages of surface modifications include:

- To prevent agglomeration by stabilizing nanoparticles.
- To increase mechanical properties by furnishing compatibility with another phase.
- To allow their self-organization.

Functionalization can also be accomplished by organic ligands which also prevents agglomeration and enable interaction of the nanoparticles with molecules, other nanoparticles, surfaces, or solids. Exchange of ligands at the surface of metal oxide NPs can be achieved without particle or particle surface, only if charge of incoming and outgoing ligands are same and same number of co-ordination sites are occupied. Metal Nanoparticles can be functionalized by thiols, disulphides, amines, nitriles, carboxylic acids and phosphines. Some of the metal oxide nanoparticle modifiers are carboxylates, silanes and phosphonates. It was found that the condensation reaction is possible on the metal oxide surface if –alkoxy or –chlorosilanes are used as organic lingand modifiers. This is because of the reaction of these functional groups in silane with –OH group on the surface of the metal oxide. It is also seen that these fuctional groups will produce HCl or alcohol as additional products which may modify the nanoparticle [6].

Corrosion is the damaging attack of a metal by its response with the surroundings. "Corrosion" alludes to the degradation of a metal by its surrounding conditions. Also, it is observed that different materials, for example, plastics, solid, wood, ceramic materials, and composite materials all experience degradation when placed in some condition [7]. Corrosion is a noteworthy test to the greater

part of the industries on the planet since it causes debacles and monstrous monetary loss. It is fundamental to recall that corrosion knows no national limits and happens both at surrounding and high temperatures. The most recent overviews show that the all out around the world, direct yearly assessed cost of corrosion (basic materials, hardware, and repair involving services, upkeep, and replacement) is roughly US$4 trillion, that is, about 4% of the country's gross domestic product (GDP). As indicated by corrosion specialists, it is conceivable to spare a net of 25% of that yearly expense by applying right now accessible corrosion control advances. Also, it is conceivable to broaden the reserve funds (up to 35%) by enhancing and applying smart coatings. In this way, there is a need to develop a viable, ecofriendly and monetarily feasible strategy for delivering and applying coatings to limit corrosion [8].

Green corrosion inhibitors are the biodegradable compounds without any heavy metals or other lethal compounds. Along with being eco-friendly and biologically acceptable, the products of plant species are of reasonable price, promptly accessible and inexhaustible. Some researchers have revealed the fruitful utilization of natural species to hinder the corrosion of metals in acidic and basic condition. For example, the extract of Delonixregia suppressed the corrosion of aluminum in hydrochloric corrosive environment, rosemary leaves were investigated as corrosion inhibitor for the Al + 2.5Mg alloy in a solution of 3% NaCl at 25◦C – etc [9].

Saeed et al., (2015) synthesized ZnO nanoparticles by direct precipitation method having pseudo spherical shape and about 20nm in average diameter as confirmed by TEM and XRD study. The uniform dispersion of polyurethane in ZnO nanoparticles (0.1-0.2wt%) was achieved by ultra-sonication to obtain ZnO Polyurethane nanocomposite (ZPN). The uniform coating was confirmed by SEM study. The ZPN was found to be more refined in terms of antimicrobial activity evaluated for Gram-negative and Gram-positive bacteria, corrosion inhibition and mechanical strength with increment in ZnO nanoparticles wt% [10]. Jothi & Palanivelu (2014) introduced an easy and economic method by developing zinc oxide nanocomposites doped with praseodymium

oxide (Pr6O11-ZnO) loaded in a hybrid sol-gel (SiOx/ZrOx) layer. The compound was studied by Transmission electron microscopy, X-Ray diffraction, X-Ray Photoelectron Spectroscopy, Fourier Transform Infrared Spectroscopy, Scanning Electron Microscopy. The compound showed universal applications like anti-corrosive nature and hydrophobic surface [11]. Behzadnasab et al., (2011) performed corrosion study of epoxy coatings comprising of different amount of amino propyl trimethoxy silane (APTES) treated ZrO2 nanoparticles. They used 3.5% NaCl solution as a media of study on mild steel surface. APS is added to ensure the dispersion of ZrO2 nanoparticles in polymer coatings. EIS, Electrochemical Noise (ECS), Salt spray test was carried out for corrosion study and found the good results for 2-3 wt% ZrO2 incorporation due to raise in barrier properties and ionic resistance [12]. Vennil & Jesurani (2017) green synthesized the face-centered cubic ZnO nanoparticles using gooseberry extract as a reducing agent and a capping agent. UV-vis absorption spectroscopy analysis showed absorption band at 390 nm. FT-IR peaks in the range of 4000-400cm-1 verified the groups like alcohol, carboxylic acid, ethers and alkenes. XRD and SEM showed the structure of nanoparticles as spherical and size range of 15 nm. Zinc and Oxide elements are confirmed by EDAX study [13]. Dehghaniet al., (2019) studied the corrosion inhibition properties of Chinese gooseberry fruit shell using two methods for mild steel in 1M hydrochloric acid media. EIS method for 1000ppm solution showed 92% inhibition efficiency. Polarization graph revealed the mixed-type inhibitor. The weight loss method showed efficiency about 94% at 25^0C for 1000ppm solution. Contact angle study indicated increased hydrophobicity. SEM, AFM also proved corrosion inhibition [14]. Nicolay et al., (2014) synthesized ZnO/sol-gel nanocomposite. Surface modification of ZnO is done by using APTES as a coupling agent. FTIR and TGA confirmed the functionalization and FEG-SEM confirmed the homogeneous dispersion of nanoparticles over the film. The information about thickness and compositions of coating were obtained by Glow discharge optical emission spectroscopy (GDOES). The compound was also studied for UV absorption and barrier effect properties using UV-Visible spectrophotometer and electrochemical impedance spectroscopy. EIS showed the good corrosion inhibition [15]. Grasset et al.,

performed the coating of commercial ZnO nanoparticles of size 20-30 nm by aminopropyltriethyloxysilane (APTES) under the conditions of acidic, basic and toluene environment to study the structural and optical properties of nanoparticles. X-ray diffraction, BET, TEM and SEM results showed that APTES is a growth inhibitor even at 800^0C [16]. Palimi et al., synthesized polyurethane-Fe2O3 nanocomposite using both modified and unmodified iron oxide nanoparticles with 3-amino propyl trimethoxy silane (APTMS). Morphology was studied by SEM. TGA and FTIR proved 5% surface grafting of APTMS. EIS and SEM was performed on steel specimens in 3.5% NaCl media and found that nanocomposites with surface modified Fe2O3 is a good corrosion inhibitor due to uniform dispersion of particles in the coating matrix, thus better coating barrier performance against electrolyte diffusion [17]. Pourhashem et al., synthesized epoxy nanocomposites using with and without amino-silane functionalized graphite oxide (GO) nanosheets. The nanosheets are incorporated in various concentration to study their action as nanofillers. FTIR, XRD, FE-SEM and EDS proved covalent grafting of (3-Aminopropyl) triethoxysilane on GO. Epoxy/silane modified GO showed good corrosion inhibition on mild steel specimen in 3.5% NaCl medium with increasing the quantity of inhibitor up to agglomeration level [18]. Jothi & Palanivelu (2013) studied the effect of silane modified nanocomposites closite 15A, MCNTs and CeCl3as corrosion inhibitor on stainless steel 304. The modification was confirmed by FTIR, XRD. SEM analysis showed the homogeneous film formation through nanocomposite intercalation. Contact angle study confirmed the hydrophobicity of surface. EIS corrosion study showed that modified $CeCl_3$is good corrosion inhibitor through anodic polarization compared to other coated and uncoated samples [19]. Javadiet al., developed nano zinc oxide particles modified by silane coupling agent and characterized the modification by TGA and FTIR. Acrylic treated ZnO nanocomposites were coated on carbon steel substrate. Up to 1wt% of nanoZnO particles, corrosion inhibition was seen through EIS method and confirmed the dispersion of nanomaterial on carbon steel and its hydrophobicity by FE-SEM, EDX and contact angle images. Photocatalytic study showed the self-cleaning property of coating surface [20]. Quadri et al., synthesized thermally stable

ZnO/polymer (PEG, PVP, and PAN) nanocomposite to study anticorrosive property on mild steel in 5% HCl media. FTIR, UV−vis, TGA and TEM techniques were performed. Potentiodynamic polarization study showed mixed-type inhibition with order of efficiency ZnO/PVP >ZnO/ PAN > ZnO/PEG and is further supported by SEM analysis [21].

2. Experimental

2.1 Chemicals & Materials

Zinc nitrate hexahydrate purchased from Sisco Research Laboratories Pvt. Ltd., N-[3-(Trimethoxysilyl)propyl]ethylenediamine purchased from Sigma-Aldrich, distilled water, PhyllanthusEmblica (Gooseberry) plant leaves.

2.2 Green synthesis of functionalized ZnO nanoparticles

50 ml of leaf extract was boiled using magnetic stirrer heater. 5g of zinc nitrate was added to the solution. To this 10 ml of N-[3-(Trimethoxysilyl)propyl]ethylenediamine was added once the precipitation is started to form. This mixture was boiled until it reduced to a deep brown colored paste. The paste was collected in a ceramic crucible and heated in muffle furnace at 4000C for 2 hours.

2.3 Characterization

2.3.1 Fourier Transform - InfraRed (FT-IR) Spectrometry

Infrared spectral study was carried out for the sample by using FT-IR spectrometer by Thermo Fischer Nicolet IS5, USA. The instrument receives broadband Near InfraRed (NIR) to Far InfraRed (FIR) spectra.

2.3.2 X-Ray powder diffraction (XRD)

X-Ray powder diffraction analysis is used to analyze the crystal structure of finely grained crystalline materials. X-Rays are illuminated using the filament kept within the tube. The current of suitable voltage (15-60 kV) is applied to produce high energetic beam of electrons and made to hit the target usually made of

copper to generate X-Rays. The diffracted beam is detected and finally processed using microprocessor.

2.4 Corrosion studies

2.4.1Potentiodynamic polarization (PDP) measurements (Tafel extrapolation method):

PDP measurements were carried out using Gill AC software. The measurements were carried out using a conventional three electrode pyrex glass cell with platinum counter electrode as auxiliary electrode and saturated calomel electrode (SCE) as reference electrode. All the values of potential are thus called SCE. Finely polished mild steel specimen (working electrode) was exposed to corrosion medium of different concentration of silane functionalized ZnO nanoparticles at different temperatures such as 30^0C, 35^0C, 40^0C, 45^0C and 50^0C. It was allowed to establish steady state open circuit potential (OCP). The polarization curves were recorded by polarizing the specimen up to -250mV cathodically and +250mV anodically with respect to OCP at scan rate of 1mVs-1. Electrochemical polarisation parameters were determined using these plots.

2.4.2 Electrochemical impedance spectroscopy (EIS) measurements

The instruments used here is the electrochemical work station, Auto Lab 30 and FRA software. In this method, a small amplitude ac signal (10mV) and frequency spectrum from 100 kHz to 0.01 Hz was applied at the OCP and impedance data was studied by plotting Nyquist. Thus, charge transfer resistance Rt was determined from the diameter of the semicircle.

2.5 Surface morphology

The SEM analysis was carried out using ULTRA 55 EVC using ZEISS technology. The surface of two mild steel sample of 1cm diameter was mirror polished. Each sample were dipped in 50ml of highest concentration inhibitor solution and blank solution for certain period of time and SEM analysis was carried out to obtain images.

3. Results & Discusiion

3.1 Characterization

3.1 Fourier transform infrared (FT-IR) spectroscopy

IR spectrum (Fig. 1.) shows the broad peak in the range of 3693 cm^{-1} to 2847 cm^{-1}, which is due to the combination absorption of N-H, C-H vibrations and also –OH group on the surface of ZnO nanoparticle. The peak at 1615cm^{-1} corresponds to N-H bending. The peak at 1029cm^{-1} corresponds to Si-O-Si stretching vibrational mode. In highly concentrated sample, the Si-O-Zn stretching will be in the range of 870cm^{-1} to 970cm^{-1} (791.62cm^{-1}). These results conclude the successful surface modification of ZnO nanoparticles [22,23,24].

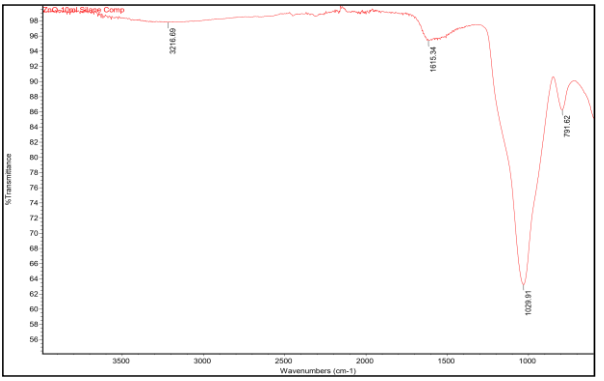

Figure. 1: FT-IR analysis of silane modified ZnO nanoparticles

3.2 X-Ray Powder Diffraction (XRD) analysis

The strong diffraction peaks (Fig. 2.) are observed corresponding to the crystal planes (100), (002), (101), (102), (110). This corresponds to the wurtzite structure of ZnO nanoparticles [25].

The Scherrer's equation applied to determine the particle size given by;

$$D = \frac{K\lambda}{\beta \cos \theta}$$

Where, D is the particle size, K = $2\sqrt{(\frac{\ln 2}{\pi})}$ =0.9 is the crystalline shape factor, λ = 1.54051 Å for Cu Kα radiation source, β is the value of full width half maxima (FWHM)

Obtained using Origin 9 software, Θ is diffracting angle in radians. By substituting the values in the above equation, the average particle size was found to be 15.5nm.

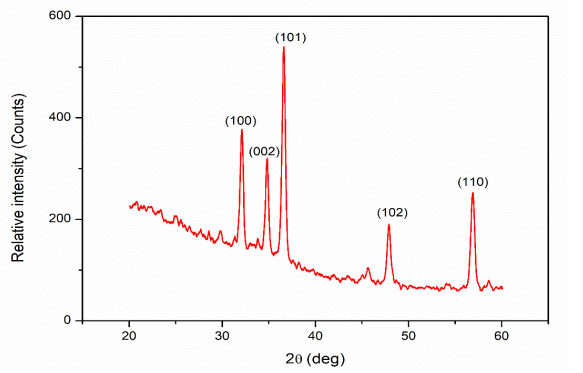

Figure. 2: XRD spectra of functionalized ZnO nanoparticle

3.3 Corrosion study

3.3.1 Potentiodynamic polarization (PDP) measurements

Fig. 3. represents the result of effect of silane/ZnO nanoparticle concentration on the cathodic and anodic polarization curves of mild steel in 0.5 HCl at 40°C and indicate that with the addition of silane modifies ZnO to 0.5M HCl solution, the polarization curves shift the anodic curves to positive potentials and cathodic curves to negative potentials compared to blank solution of 0.5M HCl. It can be concluded that both anodic metal dissolution reaction and cathodic hydrogen evolution reaction are retarded. The adsorption of Silane/ZnO on anodic and cathodic sites creates the charge transfer mechanism and is responsible for the inhibition of anodic and cathodic reactions of corrosion phenomenon.

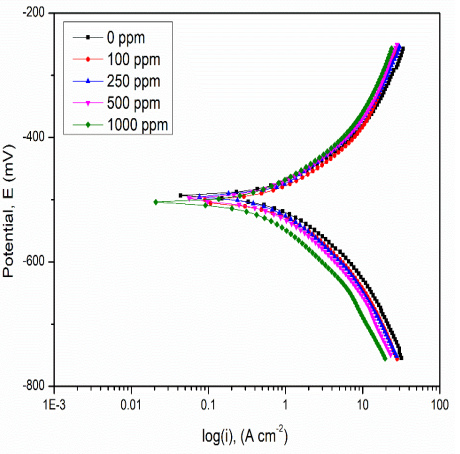

Figure. 3:Tafel polarization of mild steel in 0.5M HCl with different concentrations of functionalized ZnO nanoparticle at 40°C

Thus, concludes that the silane modified ZnO nanoparticle acts as mixed type of inhibitor. The potentiodynamic polarization parameters such as corrosion current density (icorr), cathodic slope (bc), anodic slope (ba) and corrosion rate (υcorr) were determined by extrapolating Tafel lines in corrosion potential for nanoparticle solutions of concentrations 100 ppm, 250 ppm, 500 ppm, 1000 ppm and also for blank solution. The inhibition efficiency is calculated using the formula;

$$\eta\ (\%) = [(i_{corr})_{blank} - (i_{corr})_{inhibitor}] \ / \ (i_{corr})_{blank}$$

The parameters are tabulated in the table 1. The corrosion current values decreased with increase in inhibitor concentration. Thus, the corrosion inhibition efficiency also increased as the concentration of inhibitor increased. This is because, corrosion inhibition efficiency is directly proportional to the amount of adsorbed inhibitor. The corrosion rate increased as the temperature of the media increased but the efficiency increased up to 40°C after which the desorption of inhibitor reduced the corrosion inhibition efficiency. The maximum inhibition efficiency of 61% is observed at 40°C for 1000ppm inhibitor in media.

Table1: Tafel polarization results for the corrosion of mild steel in 0.5M HCl in the presence of different concentrations of functionalized ZnO nanoparticles

Temperature of medium (°C)	Concentration(ppm)	i_{corr}(mA/cm²)	b_c(mV)	b_a(mV)	υ_{corr}(mm/yr)	ŋ (%)
	0	2.0217	192.11	161.75	23.896	
	100	1.6513	179.36	151.68	19.518	18.32
30	250	1.4514	182.67	146.84	17.155	28.21
	500	1.2669	173.8	143.89	14.975	37.33
	1000	1.0116	175.63	142.85	11.957	49.96
	0	2.8477	204.95	173.14	33.659	
	100	1.7257	181.14	127.01	20.397	39.40
35	250	1.4883	176.34	148.31	17.591	47.74
	500	1.3273	180.15	136.37	15.688	53.39
	1000	1.1739	176.17	135.69	13.875	58.78
	0	3.0741	220.33	168.39	36.335	
	100	1.7853	170.09	151.63	21.102	41.92
40	250	1.4857	164.86	130.92	17.56	51.67
	500	1.3453	154.04	121.74	15.901	56.24
	1000	1.23	156.91	121.9	14.538	61.17
	0	3.8297	205.06	140.13	45.267	
	100	2.549	163.23	139.86	29.542	33.44
45	250	2.1883	151.79	106.23	25.865	42.86
	500	1.9044	147.23	110.56	22.51	50.27
	1000	1.5968	146.95	146.44	18.874	58.30
	0	4.3101	171.66	133.29	49.954	29.10
	100	3.0558	164.25	130.91	35.416	39.48
	250	2.6084	143.05	119.21	30.231	48.07
	500	2.2381	140.39	120.41	26.454	58.14
50	1000	1.8041	156.58	129.97	20.909	

3.3.2 Electrochemical impedance spectroscopy (EIS) measurements

EIS method reveals about surface properties of the system to be examined and also the kinetics of the electrode process. The mechanistic details can be obtained by the shape of the impedance curve. Electrochemical impedance measurements in the frequency range of 105Hz - 0.01 Hz at OCP were carried out for the solution of 0.5M HCl with nanoparticles of different concentrations (0 ppm, 100 ppm, 250 ppm, 500 ppm, 1000 ppm) at temperatures 30°C, 35°C, 40°C, 45°C, 50°C. The fig 3.3 is the nyquist plots at 40°C showing the impedance behavior of mild steel in inhibitor solutions of different concentrations. The fig. 4. shows that the diameter of

the semicircle which corresponds to capacitive loop increases with the concentration of inhibitor in the electrolyte. This is the clear indication of increased corrosion inhibition in the presence of inhibitor. The electrochemical parameters are obtained from the EIS measurements and corrosion inhibition efficiency is calculated using Rct values as;

$$\eta\ (\%) = [(R_{ct})_{\text{inhibitor}} - (R_{ct})_{\text{blank}} / (R_{ct})_{\text{inhibitor}}$$

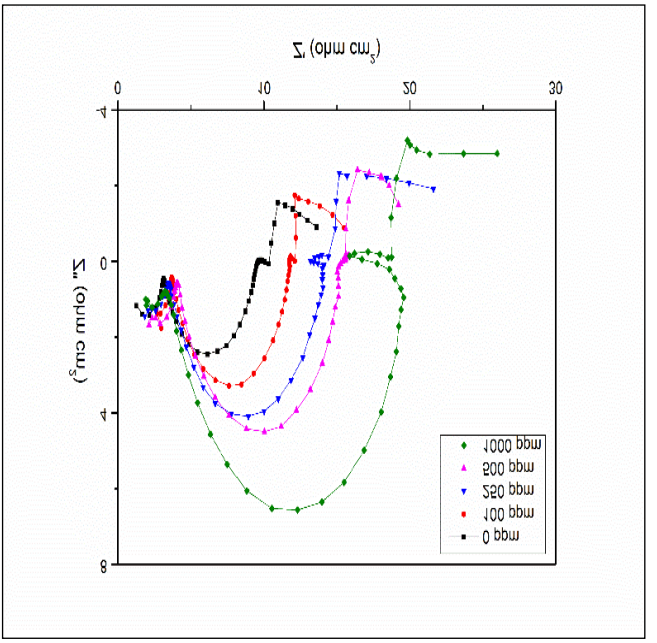

Figure. 4. Nyquist plots for mild steel in 0.5M HCl with different concentrations of Functionalized ZnO nanoparticles at 40°C

The obtained data was tabulated in Table 2. The values of polarization resistance or charge transfer resistance increases with increase in concentration of inhibitor thereby increasing the corrosion inhibition efficiency. This is because of increased adsorption of inhibitor on electrode surface with increased inhibitor concentration. The maximum inhibition efficiency of 63% is obtained at 40°C for 1000ppm inhibitor in acid media. The efficiency decreases on further rise in temperature due to desorption of inhibitor [26].

Table 2: EIS results for corrosion of mild steel in 0.5M HCl in the presence of different concentrations of inhibitor

Temperature of medium (°C)	Concentration (ppm)	R_s (Ω cm²)	R_{ct} (Ω cm²)	η (%)
	0	3.31	9.71	
	100	3.17	9.80	0.88
30	250	4.25	10.41	6.70
	500	4.14	21.16	54.10
	1000	4.45	25.17	61.41
	0	3.94	8.29	
	100	2.96	9.76	15.05
35	250	3.93	10.36	19.94
	500	3.55	18.91	56.14
	1000	3.38	22.75	63.54
	0	2.97	6.43	
	100	3.56	8.38	23.31
40	250	3.30	10.31	37.66
	500	3.76	14.82	56.63
	1000	3.02	17.89	64.07
	0	2.41	5.59	
	100	2.45	7.18	22.14
45	250	2.17	8.45	33.78
	500	2.64	10.79	48.16
	1000	2.71	15.07	62.88
	0	2.51	3.57	
	100	2.66	4.56	21.72
50	250	2.37	5.22	31.62
	500	2.81	5.78	38.29
	1000	2.72	9.23	61.34

3.4 Effect of temperature

The effect of temperature on corrosion process can be explained by using Arrhenius and Transition state equations given below respectively.

$$\ln (CR) = (-E_a/RT) + \ln A$$

$$CR = \left(\frac{RT}{Nh}\right) e^{(\Delta S^*/R)} e^{(-\Delta H^*/RT)}$$

Where CR is the corrosion rate, Ea is apparent activation energy, A is pre-exponential factor, ΔH* is the apparent enthalpy of

activation, ΔS* is the apparent entropy of activation, h is the Plank's constant (6.626x10-34 J sec mol-1), R is gas constant(8.314 J mol-1 K) and N is the Avogadro's number (6.022x1023 molecule mol-1) [27].

Arrhenius plots for the mild steel in 0.5M hydrochloric acid in the presence of different concentrations of inhibitor are shown in fig. 5. The transition state plots of ln(CR/T) versus 1/T for the mild steel in hydrochloric acid media in the presence of different concentration of inhibitor is shown in fig. 6.

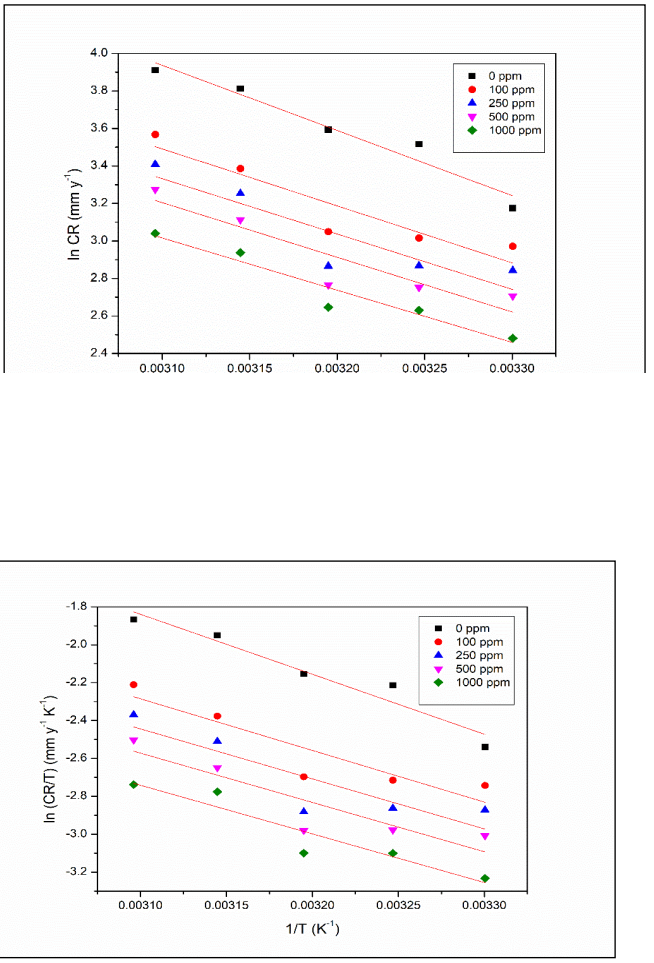

Figure. 6: plots of ln (CR/T) vs 1/T for the corrosion of mild steel in 0.5M HCl in the presence of different concentrations of silane functionalized ZnO nanoparticles

The activation parameters Ea is calculated from Arrhenius plot and ΔH*, ΔS* were calculated using transition state plots and are given in the table 3. The values of activation energy decreased in the presence of inhibitor when compared to non-inhibited solution. This may be attributed to increased corrosion inhibition efficiency with increased temperature and supports chemical adsorption of inhibitor molecules on the metal surface. Positive values of ΔH* indicates endothermic reaction i.e., metal dissolution reaction is difficult and the further decrease in value indicates the retard in metal dissolution process. The negative entropy indicates that rate determining step for activation complex is association.

Table 3: Activation parameters for the corrosion of mild steel in the presence of different concentrations of inhibitor

Activation parameters	**Inhibitor concentration (ppm)**				
	0	**100**	**250**	**500**	**1000**
E_a (kJ mol^{-1})	28.9	25.3	24.5	24.2	23.1
ΔH^* (kJ mol^{-1})	26.3	22.7	21.9	21.6	21.3
ΔS^* (J K^{-1} mol^{-1})	-131.3	-146.3	-149.8	-151.8	-154.2

3.5 Adsorption isotherms

The corrosion inhibition mechanism involves the phenomenon of adsorption of inhibitor molecules on the metal surface which depends on the factors such as charge, nature and electronic properties of the metallic surface, solvent and other ionic species adsorption, temperature of corrosion reaction and the electrochemical potential at solution interface. Adsorption isotherms are used to determine the adsorption mechanism. Langmuir adsorption isotherm was examined to fit experimental data which follows the equation;

$$\frac{Cinh}{\theta} = \frac{1}{Kads} + C_{inh}$$

Kads is the equilibrium constant for adsorption-desorption process, Θ = (ŋ/100) is the degree of surface coverage and Cinh is the concentration of inhibitor in the bulk solution. The plot of Cinh/Θ versus Cinh is the straight line (r2~0.9) with slopes nearly unity was shown in fig. 7. Standard free energy of adsorption (ΔG°ads) is related to Kads by the following equation;

ΔG°ads = - RT ln (55.5 * Kads); Where R is molar gas constant, T is absolute temperature, 55.5 is the concentration of water in solution in mol/L. The values of Kads and free energy of adsorption (ΔG°ads) for different temperature were tabulated in the table 4.

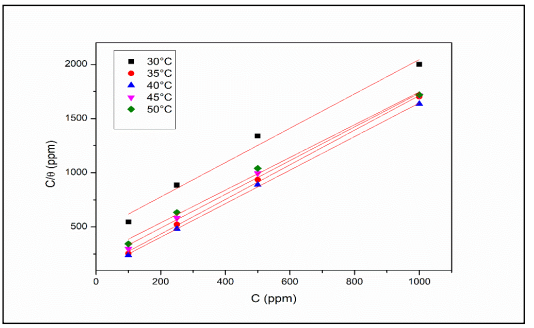

Figure. 7. Langmuir adsorption isotherm for adsorption of silane functionalized ZnO nanoparticles on mild steel in 0.5M HCl

Table 4:Calculated parameters for Langmuir adsorption isotherm

Temperature (°C)	**K_{ads} (mol^{-1})**	**$\Delta G°_{ads}$ (kJ mol^{-1})**	**R^2**
30	659.81	-26.472	0.98
35	2651.88	-30.471	0.99
40	3178.24	-31.4368	0.99
45	1706.43	-30.2947	0.99
50	1284.43	-30.0081	0.99

The value of Kads increased up to 40°C indicating adsorption process. Further increase in temperature causes desorption process and hence the value of Kads starts decreasing. The negative value of ΔG°ads indicates the spontaneous adsorption process and the stability of adsorbed layer on the surface of mild steel. The values in between -20 KJ mol-1 to -40 KJ mol-1indicates both physical adsorption and chemical adsorption process. ΔG°ads values increase up to 40°C and then decreases indicating the process of desorption [28, 29, 30, 31].

3.6 Surface morphology

From the fig. 8. on comparing sample in blank media and in media with inhibitor, corrosion is reduced and thus can be concluded that the synthesized nanoparticle is efficient as corrosion inhibitor.

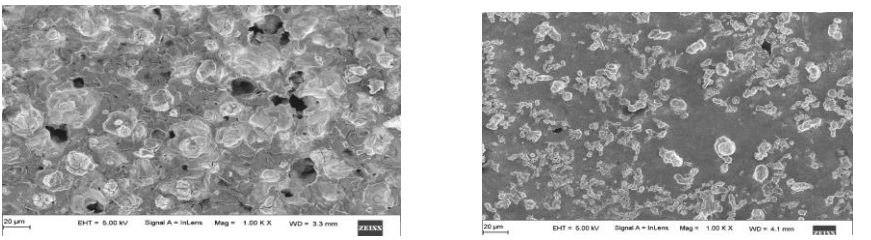

a) b)

Figure. 8. SEM image of surface of mild steel after immersion for 4h in a) 0.5M HCl medium without inhibitor b) 0.5M HCl medium with 1000ppm inhibitor

4. Conclusion

- The silane functionalised ZnO nanoparticles were synthesized using green synthesis method using PhyllanthusEmblica (Gooseberry) leaves and zinc nitrate as precursor.
- Functionalization of ZnO nanoparticles was confirmed by FT-IR technique.
- The nanorange of synthesized nanoparticles were confirmed by XRD spectral analysis. The average particle size was found to be 15.5nm.
- ZnO/silane inhibit the corrosion of mild steel in 0.5M HCl and found to be more affective.
- The corrosion inhibition efficiency increases with increase in concentration up to 1000 ppm even at high temperatures up to 50°C.
- Inhibition efficiency increased with increase in temperature up to 40°C to attain maximum value of 64% in electrochemical impedance spectroscopy technique and 61% in Tafel extrapolation technique.

- Potentiodynamic polarization measurements confirmed that the synthesized silane functionalised ZnO nanoparticles act as mixed inhibitor by inhibiting both cathodic and anodic reactions occurring in corrosion media.
- The adsorption of inhibitor on the mild steel surface obeyed Langmuir adsorption isotherm model.
- The free energy of adsorption proved the spontaneous adsorption of inhibitor on mild steel surface. The values are in the range which corresponds to both physical and chemical adsorption. This can be attributed to physical adsorption at room temperature and chemical adsorption at higher temperature.
- The activation parameters were determined using Arrhenius plot. The decrease in activation energy of inhibited solution compared to non-inhibited solution confirms the chemical adsorption process this corresponds to increase in corrosion inhibition efficiency with increase in temperature.
- SEM results of mild steel surface also confirmed silane modified ZnO nanoparticles as corrosion inhibitors.

References

[1] Bhushan, B. (2017). "Introduction to nanotechnology." Springer handbook of nanotechnology., 1-19.

[2] Mohanraj, V. J., and Chen, Y. (2006). "Nanoparticles-a review." Tropical journal of pharmaceutical research.,5, 561-573.

[3] Sirelkhatim, A., Mahmud, S., Seeni, A., Kaus, N. H. M., Ann, L. C., Bakhori, S. K. M., ... and Mohamad, D. (2015). "Review on zinc oxide nanoparticles: antibacterial activity and toxicity mechanism." Nano-Micro Letters.,7, 219-242.

[4] Simonis, M. F., and Schilthuizen, S. F. (2009). Nanotechnology: innovation opportunities for tomorrows defence. TNO.

[5] Mout, R., Moyano, D. F., Rana, S., and Rotello, V. M. (2012). "Surface functionalization of nanoparticles for nanomedicine." Chemical Society Reviews.,41, 2539-2544.

[6] Neouze, M. A., and Schubert, U. (2008). "Surface modification and functionalization of metal and metal oxide nanoparticles by organic ligands." MonatsheftefürChemie-Chemical Monthly., 139, 183-195.

[7] Andrade, C., and Alonso, C. (1996). "Corrosion rate monitoring in the laboratory and on-site." Construction and Building Materials.,10, 315-328.

[8] Gurrappa, I., and Yashwanth, I. V. S. (2015). "The importance of corrosion and the necessity of applying intelligent coatings for its control." Intelligent Coatings for Corrosion Control., 17-58.

[9] Rani, B. E., and Basu, B. B. J. (2012). "Green inhibitors for corrosion protection of metals and alloys: an overview." International Journal of corrosion.,2012.

[10] El Saeed, A. M., El-Fattah, M. A., and Azzam, A. M. (2015). "Synthesis of ZnO nanoparticles and studying its influence on the antimicrobial, anticorrosion and mechanical behavior of polyurethane composite for surface coating." Dyes and Pigments.,121, 282-289.

[11] Jothi, K. J., and Palanivelu, K. (2014). "Facile fabrication of core–shell Pr6O11-ZnO modified silane coatings for anti-corrosion applications." Applied Surface Science.,288, 60-68.

[12] Behzadnasab, M., Mirabedini, S. M., Kabiri, K., and Jamali, S. (2011). "Corrosion performance of epoxy coatings containing silane treated ZrO2 nanoparticles on mild steel in 3.5% NaCl solution." Corrosion Science.,53, 89-98.

[13] Sastry, A. B. S., Aamanchi, R. K., Prasad, C. S. R. L., and Murty, B. S. (2013). "Large-scale green synthesis of Cu nanoparticles." Environmental chemistry letters.,11, 183-187.

[14] Dehghani, A., Bahlakeh, G., and Ramezanzadeh, B. (2019). "A detailed electrochemical/theoretical exploration of the aqueous Chinese gooseberry fruit shell extract as a green and cheap corrosion inhibitor for mild steel in acidic solution." Journal of Molecular Liquids.,282, 366-384.

[15] Nicolay, A., Lanzutti, A., Poelman, M., Ruelle, B., Fedrizzi, L., Dubois, P., and Olivier, M. G. (2015). "Elaboration and

characterization of a multifunctional silane/ZnO hybrid nanocomposite coating." Applied surface science.,327, 379-388.

[16] Grasset, F., Saito, N., Li, D., Park, D., Sakaguchi, I., Ohashi, N., ... and Duguet, E. (2003). "Surface modification of zinc oxide nanoparticles by aminopropyltriethoxysilane." Journal of Alloys and Compounds.,360, 298-311.

[17] Palimi, M. J., Rostami, M., Mahdavian, M., and Ramezanzadeh, B. (2015). "A study on the corrosion inhibition properties of silane-modified Fe2O3 nanoparticle on mild steel and its effect on the anticorrosion properties of the polyurethane coating." Journal of Coatings Technology and Research.,12, 277-292.

[18] Fontana, M. G. (2018). Corrosion engineering, Third edition, McGraw-Hill, New York.

[19] Jothi, K. J., and Palanivelu, K. (2013). "Synergistic effect of silane modified nanocomposites for active corrosion protection." Ceramics International.,39, 7619-7625.

[20] Javadi, E., Ghaffari, M., Bahlakeh, G., & Taheri, P. (2019). "Photocatalytic, corrosion protection and adhesion properties of acrylic nanocomposite coating containing silane treated nano zinc oxide: A combined experimental and simulation study." Progress in Organic Coatings.,135, 496-509.

[21] Quadri, T. W., Olasunkanmi, L. O., Fayemi, O. E., Solomon, M. M., and Ebenso, E. E. (2017). "Zinc oxide nanocomposites of selected polymers: synthesis, characterization, and corrosion inhibition studies on mild steel in HCl solution." ACS omega.,2, 8421-8437.

[22] Mallakpour, S., and Madani, M. (2012). "Use of silane coupling agent for surface modification of zinc oxide as inorganic filler and preparation of poly (amide-imide)/zinc oxide nanocomposite containing phenylalanine moieties." Bulletin of materials Science., 35, 333-339.

[23] Babu, B. C., Naresh, V., Prakash, B, J., and Buddhudu, S. (2011). "Structural, thermal and dielectric properties of lithium zinc silicate ceramic powders by sol-gel method." Ferroelectrics Letters section., 38, 114-127.

[24] Abdolmaleki, A., Mallakpour, S., and Borandeh, S. (2010). "Effect of silane-modified ZnO on morphology and properties of bionanocomposites based on poly (ester-amide) containing tyrosine linkages." Polymer bulletin., 69, 15-28.

[25] Talam, S., Karumuri, S. R., and Gunnam, N. (2012). "Synthesis, characterization, and spectroscopic properties of ZnO nanoparticles." ISRN Nanotechnology.,2012.

[26] John, S., Joseph, A., Jose, A. J., and Narayana, B. (2015). "Enhancement of corrosion protection of mild steel by chitosan/ZnO nanoparticle composite membranes." Progress in Organic Coatings.,84, 28-34.

[27] Yaro, A. S., Wael, R. K., and Khadom, A. A. (2010). "Reaction kinetics of corrosion of mild steel in phosphoric acid." Journal of the University of Chemical Technology and Metallurgy.,45, 443-448.

[28] Singh, A. K., Shukla, S. K., Singh, M., and Quraishi, M. A. (2011). "Inhibitive effect of ceftazidime on corrosion of mild steel in hydrochloric acid solution." Materials Chemistry and Physics.,129(1-2), 68-76.

[29] Popova, A., Sokolova, E., Raicheva, S., and Christov, M. (2003). "AC and DC study of the temperature effect on mild steel corrosion in acid media in the presence of benzimidazole derivatives." Corrosion science.,45, 33-58.

[30] Touhami, F., Aouniti, A., Abed, Y., Hammouti, B., Kertit, S., Ramdani, A., and Elkacemi, K. (2000). "Corrosion inhibition of armco iron in 1 M HCl media by new bipyrazolic derivatives." Corrosion science.,42, 929-940.

[31] Ganash, A. A. (2019). "Comparative Evaluation of Anticorrosive Properties of Mahaleb Seed Extract on Carbon Steel in Two Acidic Solutions." Materials.,12, 3013.